

Time corrections to teleseismic P delays derived from SKS splitting parameters and implications for western U.S. P-wave tomography

Leland J. O'Driscoll,¹ Eugene D. Humphreys,¹ and Brandon Schmandt¹

Received 25 July 2011; revised 2 September 2011; accepted 6 September 2011; published 11 October 2011.

[1] Upper mantle anisotropy will affect teleseismic P-wave arrival times and create artifacts in isotropic travel-time tomography. Compiled SKS splitting results indicate variations in the strength and orientation of azimuthal anisotropy beneath the western U.S. We use SKS splitting parameters and a hexagonally anisotropic elastic tensor (fast symmetry axis) to estimate azimuthal anisotropy contributions to P-wave delay times and evaluate the effects on isotropic P-wave tomography. Estimated anisotropy correction times have a root-mean-square (RMS) value of 0.16 s, which is 37% of P-wave delay time RMS. The magnitude of azimuthal anisotropy, rather than its azimuth, has the strongest effect on P delay times; however, if the anisotropy symmetry axis has a plunge, P-wave travel times may be strongly affected by both magnitude and azimuth. Applying azimuthal anisotropy corrections significantly increases tomographic P-wave velocity beneath the High Lava Plains and central California coast, and decreases velocity beneath the Great Basin. **Citation:** O'Driscoll, L. J., E. D. Humphreys, and B. Schmandt (2011), Time corrections to teleseismic P delays derived from SKS splitting parameters and implications for western U.S. P-wave tomography, *Geophys. Res. Lett.*, 38, L19304, doi:10.1029/2011GL049031.

1. Introduction

[2] Although upper mantle anisotropy is common, as observed by its effects on surface waves and the splitting of S body waves, its effect on P-wave arrival times usually is ignored when tomographically inverting these times for structure [Sobolev *et al.*, 1999]. Babuska *et al.* [1984] suggested characterizing lithospheric anisotropy by analyzing systematic variation in P-wave travel time residuals. Joint inversion of these P-wave residuals with SKS splitting observations [Plomerova *et al.*, 1996; Babuska *et al.*, 2008] can provide constraint on three-dimensional anisotropic structure, and provide context for the similarities and differences between P- and S-wave anisotropic wave propagation. In well-studied areas such as the western U.S., observations on upper mantle anisotropy now are complete enough to allow for quantitative accounting of their effects on teleseismic P-wave arrival times. For this purpose, the most complete and useful data on upper mantle anisotropy are the split times and fast-axis orientations of SKS waves (e.g., Liu [2009], shown in Figure 1). Because SKS waves arrive with a steep inclination and are polarized in a nearly horizontal direction, the information they carry on anisotropy is limited to the elastic parameters that are sensitive to shear across a horizontal

plane. Azimuthal anisotropy is thought to be the strongest part of upper mantle anisotropy in areas where horizontal flow is dominant [e.g., Vinnik *et al.*, 1989], and P waves will be delayed where this is the case. However, development of radial anisotropy near regions of vertical flow [Panning and Romanowicz, 2006] may cause a steeply inclined anisotropic fast axis, and then a strong P-wave advance and reduced SKS split times will result [Schulte-Pelkum and Blackman, 2003]. In transitional areas a fast-axis plunge can create complicated effects [e.g., Plomerova *et al.*, 1996].

[3] In this paper, we calculate a relation between SKS split time and the resulting P-wave travel-time correction assuming azimuthal anisotropy. We then use the splitting parameters derived from SKS arrivals recorded in the western U.S. to correct teleseismic P-wave arrival times for the effects of this anisotropy. Rather than following the joint inversion method of Plomerova *et al.* [1996], we use the observed shear wave splitting field to scale the P-wave travel time through the same volume of mantle. The RMS of the travel-time corrections (0.16 s) is 37% of the data RMS, resulting in correction values large enough to change the form of tomographic inversions. Anisotropy not revealed by SKS splits is more difficult to resolve, but its effects on P delays may be even larger than those caused by azimuthal anisotropy.

2. Teleseismic P-Wave Correction Times Based on SKS Splitting Parameters

[4] Anisotropy of upper mantle peridotite has approximately hexagonal symmetry with a single fast axis. This characterization commonly is made because we typically cannot resolve any higher-order symmetry [Becker *et al.*, 2006], and the two slower axes tend to form a girdling pattern around the fast axis [Ismail and Mainprice, 1998] that has the effect of creating hexagonal symmetry. We follow Browaeys and Chevrot [2004] and decompose an olivine elastic tensor into an isotropic tensor plus a hexagonal perturbation tensor (units given in GPa),

$$\begin{aligned}
 C_{mn} = & \begin{matrix} 195 & 67 & 67 & 0 & 0 & 0 & -22 & 2 & -9 & 0 & 0 & 0 \\ 67 & 195 & 67 & 0 & 0 & 0 & 2 & -22 & 67 & 0 & 0 & 0 \\ 67 & 67 & 195 & 0 & 0 & 0 & + & -9 & 67 & 77 & 0 & 0 & 0 \\ 0 & 0 & 0 & 64 & 0 & 0 & & 0 & 0 & 0 & -3 & 0 & 0 \\ 0 & 0 & 0 & 0 & 64 & 0 & & 0 & 0 & 0 & 0 & -3 & 0 \\ 0 & 0 & 0 & 0 & 0 & 64 & & 0 & 0 & 0 & 0 & 0 & -12 \end{matrix} \\
 & \quad . \tag{1}
 \end{aligned}$$

¹Department of Geological Sciences, University of Oregon, Eugene, Oregon, USA.

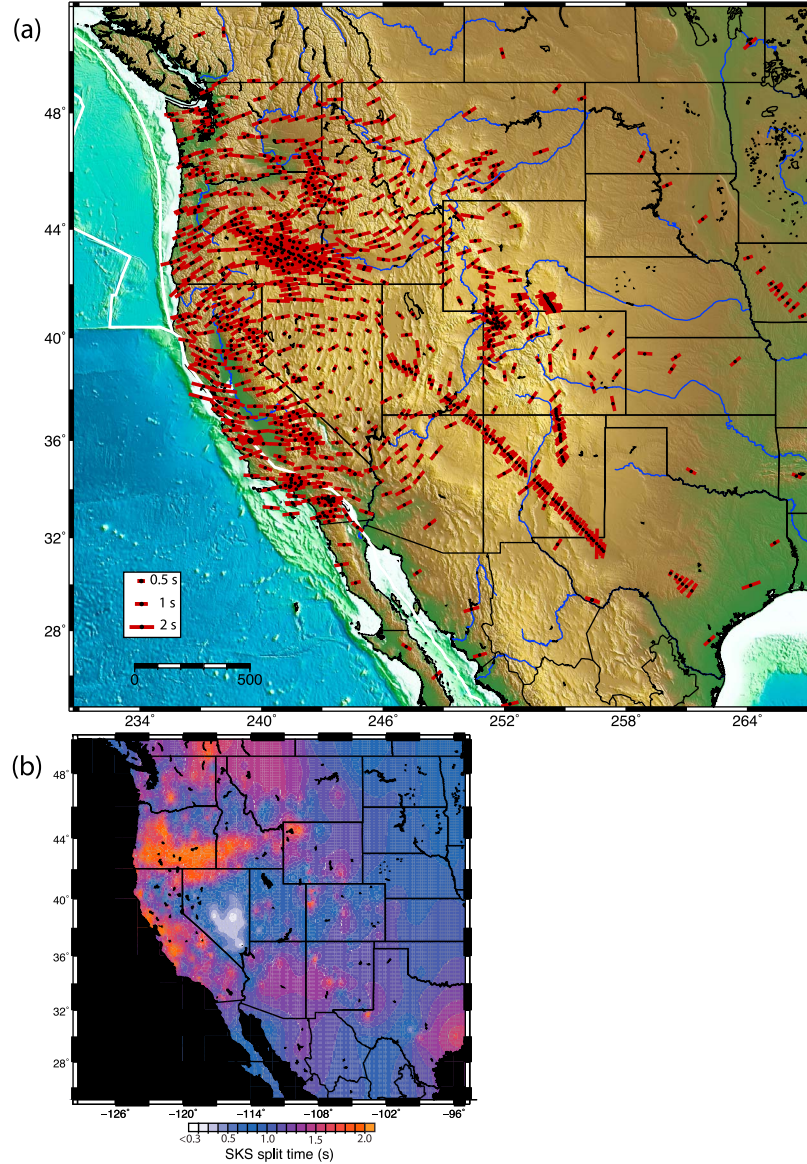


Figure 1. SKS field for the western U.S. Data compiled from Liu [2009], Long et al. [2009], West et al. [2009], Eakin et al. [2010], Wang et al. [2008], and Satsukawa et al. [2010]. (a) Station-averaged SKS split times (bar length, see key) and fast-axis orientations. (b) Interpolated SKS split-time magnitude, highlighting regions of strong splitting (e.g., High Lava Plains, southern Oregon) and minor splitting (central Great Basin, NV).

[5] We use the Voigt notation $C_{mn} = c_{ijkl}$ where the subscripts on C represent elements of the elastic tensor c_{ijkl} following the convention for m and n : $1 = >11$, $2 = >22$, $3 = >33$, $4 = >23$ or 32 , $5 = >13$ or 31 , and $6 = >12$ or 21 (e.g., $C_{44} = c_{2323}$ and also c_{3232}). The 3-axis is the fast axis. The effect of mixing olivine with orthopyroxene is well approximated simply by reducing the values in the hexagonal tensor [Browaeys and Chevrot, 2004]. The elastic constants in (1) are derived from lab experiments conducted at low pressure and temperature. There is a diminishing dominance of the hexagonal tensor over orthorhombic tensor occurs with depth, although, the hexagonal tensor of anisotropy remains stronger than the orthorhombic across the upper mantle [Browaeys and Chevrot, 2004]. All this is to say that our assumption of hexagonal symmetry captures the first-order effects of upper mantle anisotropy, and speaking practically, it is the best we can do in most situations.

[6] To calculate travel time effects on teleseismic P arrivals, we further assume an upper mantle anisotropy with a horizontal fast axis (i.e., azimuthal anisotropy). The basis for this assumption is that with SKS observations we have insufficient information that can be used to recognize or constrain the angle of dip, and hence our assumption is the one of least bias. We discuss the implications of this assumption below.

[7] With our representation of upper mantle anisotropy we now can calculate its effects on P-wave travel time. Compared to an isotropic mantle given by the isotropic elastic tensor in (1), a given teleseismic P-wave will be delayed by the presence of azimuthal anisotropy. Per unit distance, the P delay of a wave passing through anisotropic mantle, relative to that through an isotropic mantle, is $(V_{\text{Panis}}^{-1} - V_{\text{Piso}}^{-1})$. Similarly, the SKS split time per unit distance is $(V_{\text{Sfast}}^{-1} - V_{\text{Sslow}}^{-1})$ for the orthogonally polarized S waves.

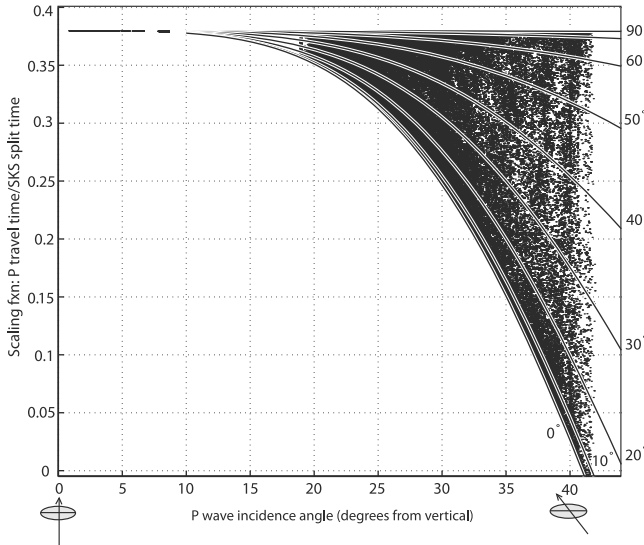


Figure 2. Ratio of P delay caused by azimuthal anisotropy to the SKS split time, as a function of P-wave incidence angle and back azimuth. Plotted curves represent the angular difference between ray back-azimuth and the SKS fast axis, ranging from 90° (ray is perpendicular to the fast axis) to 0° (ray in the vertical plane containing the fast axis, and approaches the fast axis with increasing incidence angle). Each dot represents one ray from our western U.S. ray set.

[8] Thus, given a split time δt_s , the corresponding P-wave correction time t_p is

$$t_p = \delta t_s [(V_{\text{Panis}}^{-1} - V_{\text{Piso}}^{-1}) / (V_{\text{Sfast}}^{-1} - V_{\text{SSlow}}^{-1})]. \quad (2)$$

The ratio in brackets is independent of degree of anisotropy or material density, and only depends on the propagation direction of the P and S waves with respect to the hexagonal tensor given in equation (1) (where, because anisotropy is weak, we assume that the difference between group and phase wave velocities is negligible). Figure 2 shows values of this ratio as a function of ray inclination angle, for various back-azimuths with respect to the fast-axis azimuth. To determine this ratio, we calculate the split time (per unit distance) for SKS arrivals of 10° incidence angle, and average these split times over all back-azimuths. P-wave delays are then calculated for specified values of incidence angle and back-azimuth. In a location where a 1 second split time is observed, a vertically arriving P-wave would experience a 0.38 second delay under our assumptions (Figure 2).

3. Western U.S. Teleseismic P-Wave Travel-Time Corrections

[9] To calculate P-wave travel-time corrections for the western U.S., we interpolate the SKS splitting parameters shown in Figure 1 onto a regular grid. Fast-axis azimuths are interpolated using the method of Hansen and Mount [1990]. Upper mantle anisotropy is represented by vertically projecting these results to depths of 100–300 km. Then a teleseismic ray set consisting of ~313,000 rays [from Schmandt and Humphreys, 2010a] is traced through this structure and net P-wave travel-time correction is integrated using equation (2). These values are plotted as points in

Figure 2 for incidence angles up to $\sim 43^\circ$, and the demeaned results are shown as a map in Figure 3. The distribution of P-wave correction times is compared to the observed P-wave delays in the inset of Figure 3. The RMS of the correction times is 0.16 s, or 37% of the P-wave delay times. A correction of 0.3 s would alter the imaged P-wave velocity by $\sim 1.2\%$ if the anisotropy were assumed to exist uniformly in a layer 200 km thick.

[10] Figure 4a shows an isotropic P-wave inversion (i.e., ignoring anisotropy effects), following Schmandt and Humphreys [2010b]. Figure 4b is the result of inverting the SKS-based P-wave corrections, with strong damping at depths shallower than 90 km and deeper than 350 km. This damping effectively forces velocity structure to be created at lower lithosphere and asthenospheric depths. Figure 4c results from a subtraction of the model in Figure 4b from that of Figure 4a. The dashed white ovals on Figure 4c highlight some areas of significantly altered velocity, where the strong SKS splitting leads to faster velocities.

[11] Figure 3 shows that SKS-based anisotropy delays define a prominent swath across the High Lava Plains of southern Oregon and the Snake River Plain of southern Idaho, where magmatism has been intense in the last 17 m.y. [Christiansen and Yeats, 1992]. Figure 4b shows that these corrections back-project constructively to depths of ~ 200 km. The Yellowstone area also shows SKS-based anisotropy delays, but these delays are imaged in the upper ~ 100 km indicating a more near-surface development of strong azimuthal anisotropy there (Figure S1 in the auxiliary material).¹ The other major area of correction delays is west-central California, and these delays also back-project constructively to ~ 200 km. This westernmost part of the North American plate is experiencing transform shear associated with the San Andreas Fault system, growing in along-strike length with the northward migration of the Mendocino Triple Junction [Atwater, 1970]. The most strongly negative P-wave corrections within the western U.S. occur beneath central Nevada, where splitting times are very small. Application of these corrections leads to slower velocities at depth (Figure 4), particularly above ~ 150 km (Figure S1). This is an area where a regional vertical flow is expected owing to subduction [Schmandt and Humphreys, 2010a], a sinking lithospheric instability [Roth et al., 2008; West et al., 2009] or an upwelling plume [Savage and Sheehan, 2000].

4. Discussion

[12] We present a P-wave travel-time correction based on SKS split times under the assumption of azimuthal anisotropy, which is thought to dominate upper mantle anisotropy away from regions of downwelling such as subduction zones. In areas of large split time observed over a range of back-azimuths, the fast axis of anisotropy is expected to be nearly horizontal, and the correction for P-wave delay probably is close to being correct. The back-azimuth dependence of this correction is then secondary to the magnitude in its effect on P-wave delay. However, when the fast axis has a moderate plunge, the effects on P-wave delays can be strongly back-azimuth dependent, and with moderate to vertical plunge the P-wave delays can be larger magnitude than those we cal-

¹Auxiliary materials are available in the HTML. doi:10.1029/2011GL049031.

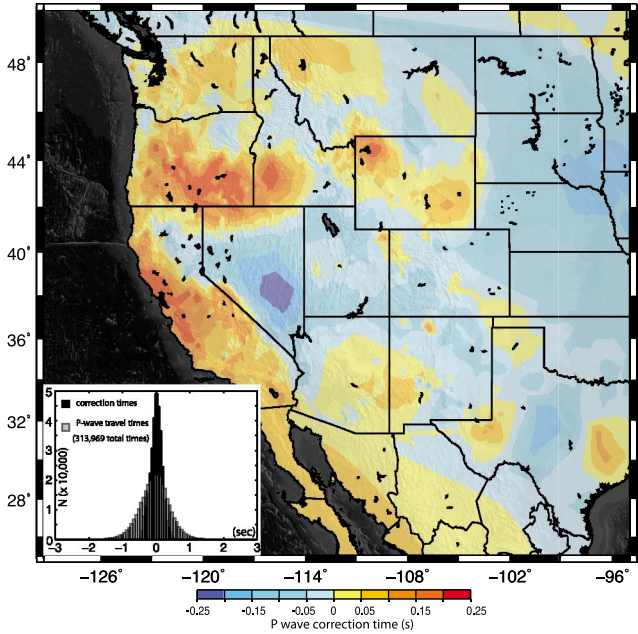


Figure 3. Interpolated map of P-wave arrival-time corrections estimated using the methods described in the text. A direct correlation between splitting magnitude and P-wave corrections is clear. (inset) Histograms of P-wave travel times (grey) and the corresponding estimated times (black) shown as dots in Figure 3. Data RMS is 0.437s, correction times RMS is 0.160s.

culate for azimuthal anisotropy [e.g., Hartog and Schwarz, 2000; Schulte-Pelkum and Blackman, 2003] (Figures S2 and S3).

[13] To illustrate the strong effect of a large fast-axis plunge angle, consider a subducted slab dipping at 55° similar to that of the imaged Gorda slab beneath northern California [Schmandt and Humphreys, 2010b; Xue and Allen, 2010;

Roth et al., 2008]. Assuming the slab has an elastic tensor fast axis that plunges at the same angle, with an average anisotropy of 5%, we can estimate the P-wave delay with respect to isotropic velocity. For waves arriving at $\pm 25^\circ$ from vertical (typical teleseismic angle of incidence at 100 km depth) and in the plane normal to the strike of the slab, the delays caused by this anisotropy are -0.38 s (raypath subparallel to slab for ~ 300 km) and 0.06 s (raypath ~ 120 km across thickness of slab). Ignoring anisotropy would tend to make the slab too fast (to account for the rays that travel up the slab) and create zones paralleling the slab that are too slow (to account for the delayed arrivals that cross the anisotropic slab and account for the delays and to compensate for a slab that is too fast). This effect may be the source of a slab-parallel slow anomaly that lies beneath the entire along-strike length of the Juan de Fuca plate [Schmandt and Humphreys, 2010b; Xue and Allen, 2010; Roth et al., 2008].

[14] With yet steeper plunge, SKS split times are small and P waves become strongly advanced. Eakin et al. [2010] discuss this correlation in the western U.S., which can be seen in Figure 4c. Thus, while split times will be small in areas where anisotropy is negligible and our calculated P-wave correction times are close to zero, regions where small splits are common also could have vertical fast axes and then the P-wave correction times should be maximal. In these cases, isotropic regions should have agreement between P and S models, whereas vertical anisotropy would create fast P-wave models compared to S-wave models. Also, nearly vertical anisotropy tends to cause S-wave splitting with a fast axis oriented toward the back-azimuth [Chevrot and van der Hilst, 2003]. This behavior is inconsistent with expectations of azimuthal anisotropy and can be mistaken for null results.

[15] To illustrate this case we assume that the elastic tensor fast axis is vertical, such as may be expected above a detached and sinking piece of lithosphere. In this case the splitting of SKS would be small and a P wave would be advanced. Assuming a 5% fast 200 km of upper mantle, a P wave with an incidence angle of 25° would be advanced by ~ 0.3 s com-

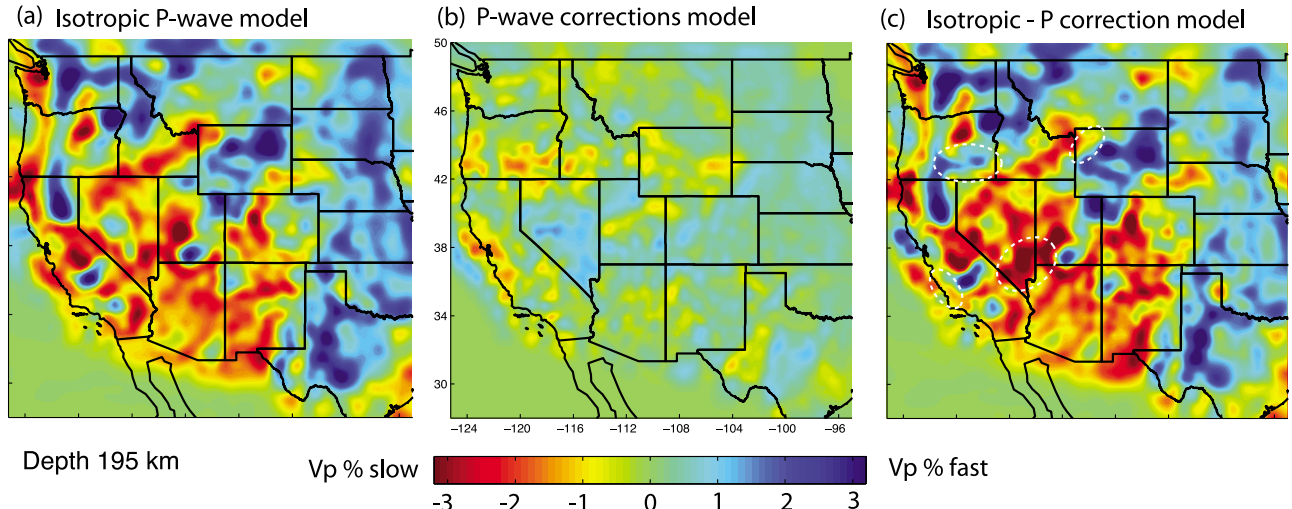


Figure 4. Comparison of velocity models at 195 km depth. (a) Isotropic inversion of western U.S. P-wave travel-time data, including crustal corrections, following Schmandt and Humphreys [2010b]. (b) Inversion of only P-wave travel-time corrections shown in Figure 3. Inversion is damped to force structure between 90 and 350 km depths. (c) Difference between the isotropic model in Figure 4a and the P delays inverted in Figure 4b. White ovals highlight regions with the most obvious change in structure from Figure 4a.

pared to the isotropic case, whereas the corresponding direct S wave would be delayed by ~ 0.3 s with respect to isotropic velocity. The result in a tomographic inversion would be a P-wave anomaly that is too fast and an S-wave anomaly that is too slow, and inconsistent estimates of SKS splitting with generally small split times. This is similar to what is imaged beneath northeast Oregon. There, a compact high-velocity structure is imaged at ~ 150 – 300 km depth that is thought to be a high-density, sinking body which is much stronger in the P-wave tomography than in the S-wave tomography [Schmandt and Humphreys, 2010a], and SKS arrivals are complex and the best-estimate split times are relatively small and fast axis azimuth is often ambiguous [Long *et al.*, 2009].

5. Conclusion

[16] We have estimated P-wave travel-time corrections based on SKS split times and applied these corrections to teleseismic P-waves recorded across the western U.S. Our considerations are limited to the effects of azimuthal anisotropy, which is thought to dominate upper mantle anisotropy away from regions of downwelling such as subduction zones. While only a part of the anisotropy effect, these correction times are significant.

[17] Horizontal anisotropy inferred from SKS does not radically change western U.S. tomography, but the effect of the P-wave correction times is significant with respect to regional variations in upper mantle velocity. There are specific areas where these differences will influence the interpretations of mantle physical state and relation of mantle structure to surface activity (e.g., volcanism). Steeply plunging anisotropy is likely in regions of subduction [Hartzog and Schwartz, 2000], plumes [Walker *et al.*, 2005], and small-scale lithospheric downwellings [e.g., Boyd *et al.*, 2004]. Hexagonal anisotropy predicts that such areas with plunging anisotropy could introduce more dramatic artifacts in isotropic travel-time tomography than those presented here.

[18] **Acknowledgments.** We thank Martha Savage and an anonymous reviewer for useful insight and helpful comments. This research was supported by NSF grants EAR-0952194 and EAR-0911006.

[19] The Editor thanks Martha Savage and an anonymous reviewer for their assistance evaluating this paper.

References

- Atwater, T. (1970), Implications of plate tectonics for the Cenozoic tectonic evolution of western North America, *Geol. Soc. Am. Bull.*, **81**, 3513–3536, doi:10.1130/0016-7606(1970)81[3513:LOPTFT]2.0.CO;2.
- Babuska, V., J. Plomerova, and J. Sileny (1984), Large-scale oriented structures in the subcrustal lithosphere of central Europe, *Ann. Geophys.*, **2**, 649–662.
- Babuska, V., J. Plomerova, and L. Vecsey (2008), Mantle fabric of western Bohemian Massif (central Europe) constrained by 3D seismic P and S anisotropy, *Tectonophysics*, **462**, 149–163, doi:10.1016/j.tecto.2008.01.020.
- Becker, T. W., S. Chevrot, V. Schulte-Pelkum, and D. K. Blackman (2006), Statistical properties of seismic anisotropy predicted by upper mantle geodynamic models, *J. Geophys. Res.*, **111**, B08309, doi:10.1029/2005JB004095.
- Boyd, O. S., C. H. Jones, and A. F. Sheehan (2004), Foundering lithosphere imaged beneath the southern Sierra Nevada, California, USA, *Science*, **305**, 660–662, doi:10.1126/science.1099181.
- Browaeys, J. T., and S. Chevrot (2004), Decomposition of the elastic tensor and geophysical applications, *Geophys. J. Int.*, **159**, 667–678, doi:10.1111/j.1365-246X.2004.02415.x.
- Chevrot, S., and R. D. van der Hilst (2003), On the effects of a dipping axis of symmetry on shear wave splitting measurements in a transversely isotropic medium, *Geophys. J. Int.*, **152**, 497–505, doi:10.1046/j.1365-246X.2003.01865.x.
- Christiansen, R. L., and R. L. Yeats (1992), Post-Laramide geology of the U.S. Cordilleran region, in *The Geology of North America*, vol. G3, *The Cordilleran Orogen: Conterminous U.S.*, edited by B. C. Burchfiel, P. W. Lipman, and M. L. Zoback, pp. 261–406, Geol. Soc. of Am., Boulder, Colo.
- Eakin, C. M., M. Obreski, R. M. Allen, D. C. Boyarko, M. R. Brudzinski, and R. Porritt (2010), Seismic anisotropy beneath Cascadia and the Mendocino triple junction: Interaction of the subducting slab with mantle flow, *Earth Planet. Sci. Lett.*, **297**, 627–632, doi:10.1016/j.epsl.2010.07.015.
- Hansen, K. M., and V. S. Mount (1990), Smoothing and extrapolation of crustal stress orientation measurements, *J. Geophys. Res.*, **95**, 1155–1165, doi:10.1029/JB095iB02p01155.
- Hartog, R., and S. Y. Schwartz (2000), Subduction-induced strain in the upper mantle east of the Mendocino Triple Junction, California, *J. Geophys. Res.*, **105**, 7909–7930, doi:10.1029/1999JB900422.
- Ismail, W. B., and D. Mainprice (1998), An olivine fabric database: An overview of upper mantle fabrics and seismic anisotropy, *Tectonophysics*, **296**, 145–157, doi:10.1016/S0040-1951(98)00141-3.
- Liu, K. H. (2009), NA-SWS-1.1: A uniform database of teleseismic shear wave splitting measurements for North America, *Geochem. Geophys. Geosyst.*, **10**, Q05011, doi:10.1029/2009GC002440.
- Long, M. D., H. Gao, A. Klaus, L. S. Wagner, M. J. Fouch, D. E. James, and E. Humphreys (2009), Shear wave splitting and the pattern of mantle flow beneath eastern Oregon, *Earth Planet. Sci. Lett.*, **288**, 359–369, doi:10.1016/j.epsl.2009.09.039.
- Panning, M., and B. Romanowicz (2006), A three-dimensional radially anisotropic model of shear velocity in the whole mantle, *Geophys. J. Int.*, **167**, 361–379, doi:10.1111/j.1365-246X.2006.03100.x.
- Plomerova, J., J. Sileny, and V. Babuska (1996), Joint interpretation of upper-mantle anisotropy based on teleseismic P-travel time delays and inversion of shear-wave parameters, *Phys. Earth Planet. Inter.*, **95**, 293–309, doi:10.1016/0031-9201(95)03122-7.
- Roth, J. B., M. J. Fouch, D. E. James, and R. W. Carlson (2008), Three-dimensional seismic velocity structure of the northwestern United States, *Geophys. Res. Lett.*, **35**, L15304, doi:10.1029/2008GL034669.
- Satukawa, T., K. Michibayashi, U. Raye, E. Y. Anthony, J. Pulliam, and R. Stern (2010), Uppermost mantle anisotropy beneath the southern Laurentian margin: Evidence from Knippa peridotite xenoliths, Texas, *Geophys. Res. Lett.*, **37**, L20312, doi:10.1029/2010GL044538.
- Savage, M. K., and A. F. Sheehan (2000), Seismic anisotropy and mantle flow from the Great Basin to the Great Plains, western United States, *J. Geophys. Res.*, **105**, 13,715–13,734, doi:10.1029/2000JB900021.
- Schmandt, B., and E. Humphreys (2010a), Complex subduction and small-scale convection revealed by body-wave tomography of the western United States upper mantle, *Earth Planet. Sci. Lett.*, **297**, 435–445, doi:10.1016/j.epsl.2010.06.047.
- Schmandt, B., and E. Humphreys (2010b), Seismic heterogeneity and small-scale convection in the Southern California upper mantle, *Geochem. Geophys. Geosyst.*, **11**, Q05004, doi:10.1029/2010GC003042.
- Schulte-Pelkum, V., and D. K. Blackman (2003), A synthesis of seismic P and S anisotropy, *Geophys. J. Int.*, **154**, 166–178, doi:10.1046/j.1365-246X.2003.01951.x.
- Sobolev, S. V., A. Grésillaud, and M. Cara (1999), How robust is isotropic delay time tomography for anisotropic mantle?, *Geophys. Res. Lett.*, **26**, 509–512, doi:10.1029/1998GL900206.
- Vinnik, L. P., V. Farra, and B. Romanowicz (1989), Azimuthal anisotropy in the Earth from observations of SKS at Geoscope and NARS broadband stations, *Bull. Seismol. Soc. Am.*, **79**, 1542–1558.
- Walker, K. T., G. H. R. Bokelmann, S. L. Klempner, and G. Bock (2005), Shear-wave splitting around the Eifel hotspot: Evidence for a mantle upwelling, *Geophys. J. Int.*, **163**, 962–980, doi:10.1111/j.1365-246X.2005.02636.x.
- Wang, X., J. F. Ni, R. Aster, E. Sandvol, D. Wilson, C. Sine, S. P. Grand, and W. S. Baldridge (2008), Shear-wave splitting and mantle flow beneath the Colorado Plateau and its boundary with the Great Basin, *Bull. Seismol. Soc. Am.*, **98**, 2526–2532, doi:10.1785/0120080107.
- West, J. D., M. J. Fouch, J. B. Roth, and L. T. Elkins-Tanton (2009), Vertical mantle flow associated with a lithospheric drip beneath the Great Basin, *Nat. Geosci.*, **2**, 439–444, doi:10.1038/ngeo526.
- Xue, M., and R. M. Allen (2010), Mantle structure beneath the western United States and its implications for convection processes, *J. Geophys. Res.*, **115**, B07303, doi:10.1029/2008JB006079.

E. D. Humphreys, L. J. O'Driscoll, and B. Schmandt, Department of Geological Sciences, University of Oregon, 1272 University of Oregon, Eugene, OR 97402, USA. (lodrisco@uoregon.edu)